Electrochemical Nb_3Sn Film Technologies

Carlo Ciaccia[1], Stefano Falletta[1], Hayato Ito[2]
[1]Supervisor: Emanuela Barzi
[2]SOKENDAI, Hayama, Kanagawa, Japan

Abstract

In recent years RF cavity performance has approached the theoretical limit for bulk Nb, and this has stimulated research in alternatives such as Nb_3Sn films. SRF cavities with a layer of Nb_3Sn coated on the inner surface have been demonstrated to improve the cavity quality factor (lower power dissipation and narrower bandwidth). From a theoretical point of view, an almost doubled accelerating gradient is also predicted, even though it has not been experimentally observed so far [1].
The aim of this report is to describe an electrochemical technique to realize superconducting Nb_3Sn films onto a Nb substrate. The original recipe was developed by FNAL in collaboration with Politecnico di Milano [2] and then optimized during a Summer School collaboration at Fermilab in 2017 [3].
Research is not ended at all. The present work wants to be the starting point for future internships on the topic. Improvements of the original recipe will be proposed along with suggestions for the directions of future research.
Different electrodes configurations were explored in order to determine their effects on the electrochemical process and to mimic the deposition on RF cavities (too expensive to be used in optimization trials).
The quality of the deposited layers and of the superconducting phase has been verified by means of SEM and EDS analysis.
The first samples that were realized turned out to be not superconducting, thus pushing us towards a better standardization and a deeper analysis of all the process parameters.

Keywords: SRF Cavities – Superconducting films – Electrodeposition – Electrodes Configuration – Thin films characterization techniques

1 INTRODUCTION

The main advantages of Nb_3Sn over Nb are related to its higher critical temperature T_c ($18.3K$ vs $9.2K$), that allows to save power dissipation related to the refrigerating system, and to its higher critical field H_{c2} ($30T$ vs $0.82T$), that allows to obtain, at least in theory, a larger accelerating gradient.
However, Nb_3Sn is a quite brittle material and its superconductivity is strain sensitive, which means that it is destroyed if a sufficiently large stress is applied.

Both Nb_3Sn and Nb are type II superconductors, which is to say that there exist two critical magnetic field thresholds. When a magnetic field in between the two thresholds is applied, the material is neither in the normal or in the superconducting state, but in a mixed state in which magnetic flux lines penetrates in the form of vortices also known as *fluxons* (fig.1). The more the material crystal structure is able to pin fluxons position, the lower is the power dissipation and the higher is the allowed current.

The pinning force of a superconductor strictly depends on the mechanical and thermal treatments performed on it, since they determine its microstructure[4]: the strongest flux pinning is achieved when the grain size is comparable to the superconductor penetration depth ($\approx$ 40nm in Nb_3Sn). In order to obtain such small grains, the temperature of the process must be as low as possible, its minimum being determined by the energy required to form the superconducting phase.

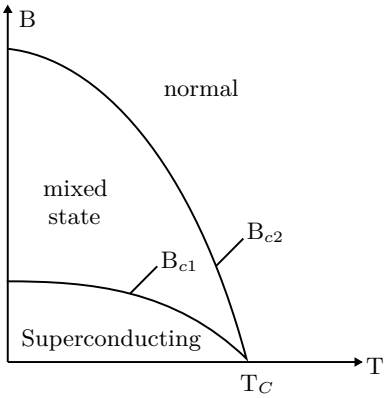

Figure 1. Typical critical fields *vs* temperature curve for a type II superconductor.

The currently most diffused deposition technique for Nb_3Sn films is Physical Vapour Deposition, which is quite slow and expensive compared to Electrodeposition, and typically requires higher temperature for film formation. The fact that the almost doubled accelerating gradient predicted by the theory has not been observed so far may be due to the large grain size obtained with PVD, even though the debate on the optimal grain size is not closed yet[1]. Therefore, electrodeposition seems to be an interesting alternative for fast and low cost coating of SRF cavities.

In the present paper a combination of thermal diffusion processes and electrochemical techniques is proposed. The superconducting phase is formed after annealing of a ternary system: an inner copper layer electrodeposited on the niobium substrate is followed by a tin layer and a copper barrier layer. Details are given in the following.

2 SUPERCONDUCTIVE PHASE FORMATION

In the binary system Nb-Sn, the Nb_3Sn phase forms alone only above $930°C$; below that temperature other non superconducting phases such as Nb_5Sn_6 and $NbSn_2$ arise [4].
That is why a ternary system Nb-Cu-Sn has been used here. Each layer is deposited by using a different electrolytic bath (details on the composition are provided in 3.1) and accomplishes a specific function:

1. The first copper layer acts as a catalyst, which means it allows to reduce the temperature of the annealing process to approximately $700°C$. It should not affect the superconducting properties of the Nb_3Sn layer and should also reduce the formation of non superconducting phases.
   Even if it is not easy to find a complete phase diagram of the ternary system Nb-Cu-Sn in literature, the above information have been confirmed by several works [2, 3, 4];
2. The tin layer is responsible for the formation of the Nb_3Sn phase. It diffuses inside the above mentioned copper layer and reacts with the niobium substrate;
3. The external copper layer is added as a barrier to prevent tin leakages and avoid formation of aggregates;

The resulting structure is shown in fig.2. The annealing process consists in three steps and lasts approximately 6 days.

In the first step the system is heated up to T_1=$206°C$ for $72h$. T_1 has been chosen slightly lower then the Sn melting point ($232°C$) to allow the relaxation of the internal stress that would be deleterious for the superconducting properties.

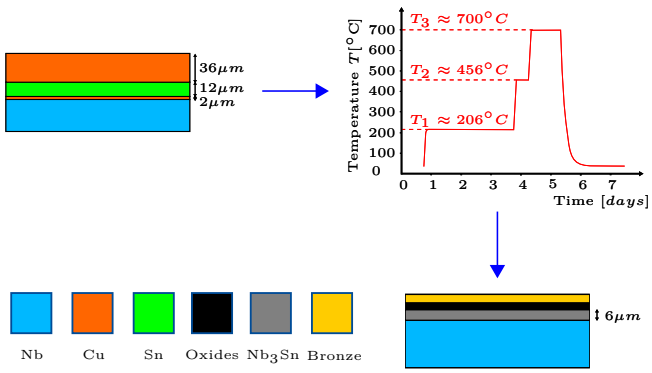

Figure 2. Schematic of the heat treatment required for the formation of the superconducting phase. The resulting undesired layer of bronze and Nb oxides on the outer surface must be removed by chemical etching or mechanical polishing for SRF applications.

In the second step the temperature is increased to $456°C$ for $10h$. During this step the liquid tin phase diffuses toward the niobium substrate and in the barrier layer. Diffusion inside the outer copper layer is responsible for the formation of a bronze layer that, for applications is superconducting cavities, must be removed through some kind of polishing - i.e. mechanical or chemical.
It is important to notice that the presence of oxides in between the layers not only degrades adhesion, but also impede the diffusion of tin. For this reason, the substrate has always been rinsed in hydrofluoric acid (49% for $5min$) before deposition steps. Also, it is highly suggested to use oxygen free electrodes and to grind them to remove spurious deposits and oxides before every step.

The third step lasts $24h$ at $700°C$ and is responsible for the formation of the superconducting phase. Because of the randomness of diffusion processes it is intuitive to expect that almost half of the deposited tin will react with the niobium substrate.

It is important to optimize the ratios between the thickness of the tin and the two copper layers. The thickness of the catalyst layer should be neither too large or too small compared to the tin layer since in both cases after diffusion and then reaction of tin, the stoichiometry of Nb_3Sn could not be respected and spurious phases would form. Based on results in [3] a ratio $t_{Sn}/t_{Cu_1} \approx 6$ has been chosen. In practice, as it will be clearer in 3.2.2, the process parameter to be varied in order control such ratio is the charge per unit area $J \cdot t$ which is applied to the substrate at each step. This is assumed to be linearly related to the thickness of the deposited layer.

To find the right value of t_{Cu_2}/t_{Sn} is instead more tricky, since the ability of the outer copper layer in preventing

[1]The other opinion is that high flux pinning is good for the realization of magnets but not for RF applications, where one must be able to reverse signal polarity quickly.

tin leakage apparently does not follow a linear trend. This is one of the possible reasons that made the first samples non superconducting. If the ratio between the outer copper layer and the tin layer is smaller than 2, than large tin/bronze aggregates will form on the outer surface after the heat treatment. This is evident in fig.3 where a cross section of sample D25[2] is shown. In this case t_{Cu_2}/t_{Sn} is ≈ 1.

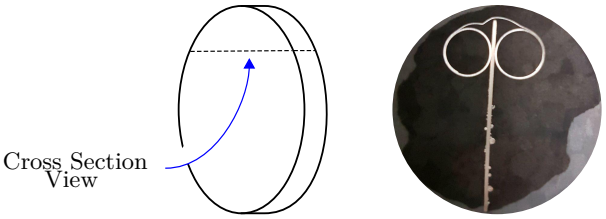

Figure 3. Cross section of sample D25 after the heat treatment. On the left an image of the mold realized for SEM observation is shown. Bubbles on the two sides of the substrate are clearly visible.

3 ELECTRO-PLATING

As stated before, electrodeposition is a relatively cheap and fast technique that allows to realize multilayered structures on virtually any substrate with a rate of a few microns per minute. A schematic of the experimental setup is shown in fig.4 for different shapes of the substrate: the electrodes configuration used for deposition on rectangles and disks is in the top of the figure while the one used for cylinders is in the bottom. Rectangles and disks were realized in order to study the electroplating process and test the superconducting properties of the Nb_3Sn[3], while deposition on cylinders was aimed to mimic conditions in SRF cavities were curved surfaces, and therefore additional stresses in the substrate, are present.

Basically, the material to be deposited is provided by the electrolytic solution, in which its ions are dissolved. When an external voltage (or current) is applied to the electrodes, ions in the solution get reduced on the cathode (substrate) forming the desired layer, while the atoms of the anode get oxidised and replenish ions concentration in the solution.
Alternatively, inert platinum anodes could be used in place of Cu and Sn electrodes. In this case the material to be deposited is still dissolved in the solution but must

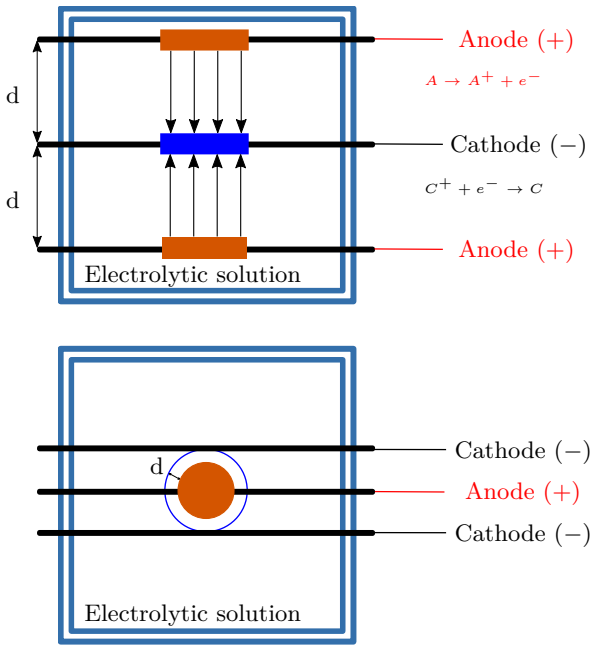

Figure 4. Electrodeposition setup. Top: electrodes configuration for deposition on disks and rectangles. Bottom: electrodes configuration for deposition on cylinders.

be periodically renewed. Here it was decided to do not use inert electrodes to avoid constant changes in the baths.
The quality of the deposit depends on a large numbers of parameters. Their effects will be addressed in the following sections along with ideas to obtain the best performance. However, an optimal recipe for the ternary system Nb-Cu-Sn is not available in literature: at present we could have found a local minimum of the multivariable functional governing the deposition process, but still the possible directions to takes are many and the global minimum (if any) is hard to be reached.

3.1 Electrolytic Solutions

Each deposition step requires a different electrolytic bath since even when the anode material is the same (first and third steps) the substrate is different (niobium and tin respectively). The composition of each bath is summarized in fig.5.
Since niobium is not a reactive metal, an acid copper solution has been chosen for the first step. The chemical cost of acid copper baths is low and they can have a wide range in composition. Compared with alkaline or mildly alkaline copper bath (see the third step) they are easier to control and are more stable, even if they have a lower throwing power. The standard solution is made by copper sulfate Cu_2SO_4 and sulfuric acid H_2SO_4. A concentration of less than $60g/L$ of copper sulfate degrades deposition efficiency, while sulfuric acid gives the baths high conductivity and

[2]The first letter indicates the shape of the substrate (R = Rectangular, D = Disk, C = Cylinder), while the number is the number of the sample. A detailed summary of the process parameters for each sample is given in Table 2.

[3]If we were able to remove the outer bronze layer without degrading the superconducting properties of the samples, Jefferson Lab would be able to provide us a measure of the quality factor that may be reached with the present technique. An estimate of the quality factor is fundamental to understand the extent of possible applications.

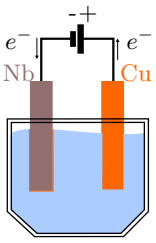

Chemical	Quantity per Litre of H_2O
H_2SO_4	230mL
$CuSO_4$	160 g

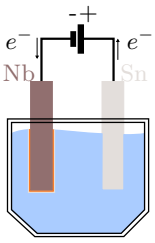

Chemical	Quantity per Litre of H_2O
Solderon Acid HC	430mL
Solderon Tin HS-300	333 mL
Solderon MHS-W	200 mL

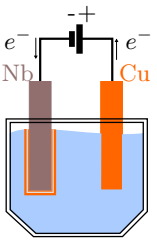

Chemical	Quantity per Litre of H_2O
$Cu_2P_2O_7$	55 g
$NaNO_3$	25 g
$Na_4P_2O_7$	400 g

Figure 5. Schematic of every deposition steps along with the description of the corresponding elecrolytic solution.

prevents the formation of insoluble salts (a practical minimum concentration is about $45g/L$). In order to increase the deposition rate [4] suggests to add HCl to the standard solution. Indeed hydrochloric acid helps the dissolution of copper, but if its concentration is too high then cuprous chloride CuCl will form on the anode preventing further deposition. Since CuCl can be toxic and the deposition rate can also be increased by increasing the current density (or reducing the electrode distance), HCl has been completely removed from the recipe and sulfuric acid has been added. Indeed H_2SO_4 increases the conductivity of the solution and therefore the maximum allowed current density (see 3.2.1).

The same idea has been used for the second step, where tin is deposited on copper. In this case however the exact content of the bath was unknown since chemicals were proprietary. Additives are used to increase the throwing power, the stability and the smoothness of the deposit. On the contrary of the other two baths, this solution never required maintenance - i.e. due to high current density burning or contamination.

The third solution is the more delicate one. Acid baths (at least[4] according to [4]) cannot be used to deposit copper on tin since they would produce non-adhering deposit. A mildly alkaline pyrophosphate copper bath is used instead: cupric pyrophosphate $Cu_2P_2O_7$ dissolves in sodium pyrophosphate $Na_4P_2O_7$ and forms a complex ion from which copper plates. Potassium, if available, may be used instead of sodium because of its higher solubility and electrical conductivity.
The presence of nitrate and an higher concentration of complex ions enhance the maximum allowable current density, and that is why the quantity of $NaNO_3$ and $Cu_2P_2O_7$ has been increased with respect to last year [3]. Indeed, this bath degrades quite easily. When this happens the solution changes color and it must be prepared again.
This solution is also the most difficult to be prepared since T>100°C is required to dissolve all the constituents.

Let's see in more details which are the main process parameters and how they affect deposition.

3.2 Process Parameters

3.2.1 Current Density

When a metal M (electrode) is immersed in an aqueous solution containing ions of that metal[5] M^{z+}, there will be an exchange of such ions between two phases, the metal and the solution. Initially, depending on the metal and on the ions concentration, one of the two reactions may occur faster than the other: as a consequence the metal side of the interface will acquire a negative (if oxidation preferred) or positive (if reduction preferred) charge that will eventually bring the system to a dynamic equilibrium:

$$M^{z+} + ze^- \leftrightarrow M \tag{1}$$

where z is the number of electrons involved in each reaction.
As a result of charging of the interface, a potential difference will arise between the metal and the solution that can be measured only with respect to another electrode (Standard Hydrogen Electrode). The resulting cell potential difference, also called equilibrium potential, depends on the ions concentration according to Nernst equation:

$$E = E^0 + \frac{RT}{zF} ln\left[a(M^{z+})\right]. \tag{2}$$

[4] We did not have time to verify this, but it could be interesting to apply the first or another non-aqueous solution to the third step. So as to avoid all problems related to the maintenance of the third solution.

[5] Here the metal is modelled as an ionic crystal surrounded by an electron gas

Here, E^0 is the relative standard electrode potential of metal M and $a(M^{z+})$ is the activity of the metal ions in the solution, which is typically approximated with the ions concentration. R,T and F are the gas constant, the temperature of the bath and the Faraday's constant respectively. The Faraday's constant represents the charge carried by a mole of electrons ($F = N_A e = 96487 C/mol$).
When an electrode is made part of an electrochemical cell through which current is flowing, its potential $E(I)$ will differ from the equilibrium potential E. The difference between these two potentials,

$$\mu = E(I) - E \tag{3}$$

is called *overpotential*.

The current-potential relationship can be divided in three regions depending on the deposition rate-determining process. A typical curve is shown if fig.6. When the deposition rate is determined by charge transfer at the interface, the current density increases exponentially with the overpotential. This goes on until mass transport limitations come in place and the current density reaches a saturation value i_L.
At values of the applied current near the limiting current

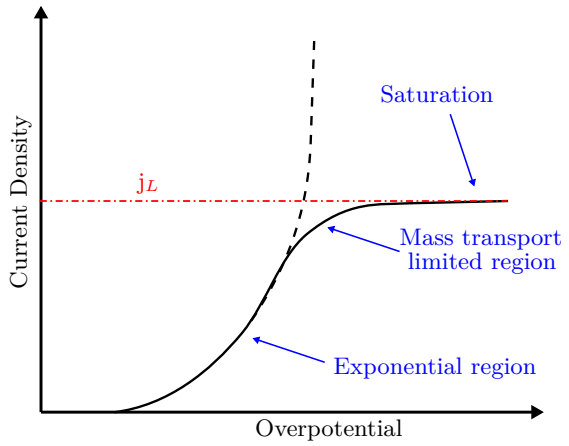

Figure 6. [5] Three regions in the general current-overpotential relationship.

density, the species M^{z+} are reduced as soon as they reach the electrode and the rate of the reaction becomes determined by the rate of transport of the ions in the solution. If an even larger external current is forced through the electrode, other process than reduction of M^{z+} will occur degrading the solution.
As it will be clearer in the next sections when discussing Faraday's law (6), increasing the current density increases the plating rate. However, Landau [6] observed that the deposit deteriorates when the current density exceeds some value depending on the solution composition and operating variables. Rough, burnt, dentritic or powdery deposits maybe obtained when the ratio of the actual plating current density to the limiting current density j/j_L exceed 0.6.
The limiting current density is given by [5]

$$j_L = \frac{zFD}{\delta} c_b, \tag{4}$$

where D is the diffusion coefficient of the depositing species and c_b is the bulk[6] concentration of ions in the solution. The most tricky parameter is the diffusion layer thickness δ, which in the Nernst diffusion model is defined as the distance from the electrode surface where the ions concentration starts falling off linearly (see fig.7). It depends on several parameters among which

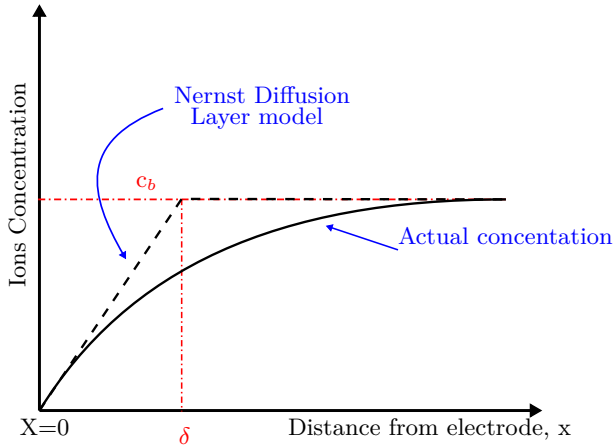

Figure 7. [5] Nernst diffusion model for the determination of the diffusion layer thickness.

the electrode material and geometry, the viscosity of the solution, the agitation and the temperature of the bath and, also, the type of applied signal.
Let us consider as an example the first solution. Assuming a diffusion coefficient of the Cu^{++} ions equal to $5\text{x}10^{-6} cm^2 s^{-1}$ [7] and a diffusion layer thickness of $10\mu m$ [8], then, since the ions concentration is equal to $0.376\text{x}10^{-5} mol/cm^3$, the limiting current density turns out to be:

$$\begin{aligned} j_L &= \frac{2 \cdot 96487 \cdot 5 \cdot 10^{-6} \cdot 0.376 \cdot 10^{-5}}{10 \cdot 10^{-4}} \text{A/cm}^2 \\ &\approx 3.62 \text{mA/cm}^2 \end{aligned} \tag{5}$$

Compared to the above value, the current densities used in our deposition steps (see Table 2) are 10 times larger, and should therefore produce poor quality deposits.

The trick lays in the fact that the diffusion layer thickness in [8] refers to the case where a DC signal is applied to the electrodes. In the present work instead, AC waveforms are used, since they are highly suggested in literature to obtain brighter and smoother deposit. Indeed, one important effect of pulsed signals is a modification

[6] Far from the electrode surface.

of the diffusion layer thickness. AC waveforms split the Nernst diffusion layer into two diffusion layers: the stationary diffusion layer and the pulsating diffusion layer. In the last, ions concentration decreases more rapidly than in the DC case, so that the average diffusion layer thickness gets reduced. As a consequence the actual limiting current density is increased and the quality of the deposit improved.
The difference between a good and a bad deposit is visible with naked eye. In fig.8 the results of the second deposition step with current densities of 50mA cm^{-2} and 35mA cm^{-2} are compared. In the first case the deposit appears much more dentritic.

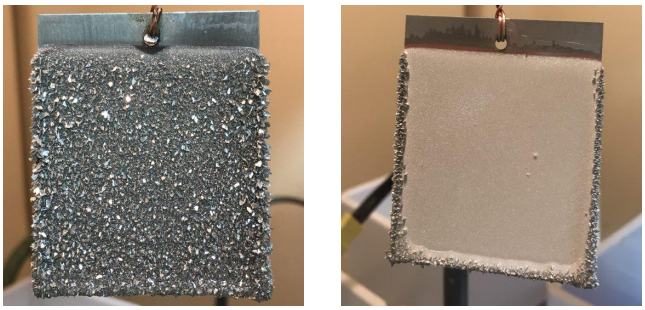

a) b)

Figure 8. a) Second step performed at 50mA cm^{-2}. b) Second step performed at 35mA cm^{-2}.

At the beginning of the project we tried different waveforms with different duty cycles (fig.9).
Since deposition of metal ions results in depletion of the solution in the region near the electrode surface, these ions must be replenished to ensure continuity in the diffusion process. The interruption or rest period of the signal is to permit the diffusion layer to be replenished. The replenishment of ions can also be accomplished by mechanical agitation of the solution and that is why the use of a magnetic stirrer during the deposition step is fundamental.

The reverse period instead should reduce the effect of current crowding avoiding bumps formation. However, since the first samples turned out to be not superconducting and no significant improvement in the deposit uniformity was observed, we decided to remove the reverse period and moved back to the recipe of last year [3]. In practice the impediment in the superconducting phase formation, which will be addressed later on, was not the reverse period and therefore it could be interesting during next years to try different duty cycles and frequencies in order to improve the deposition process[7].
All the subsequent samples were realized using just an

[7] [9] suggests 10–60 sec direct current followed by 2–20 sec of reverse current.

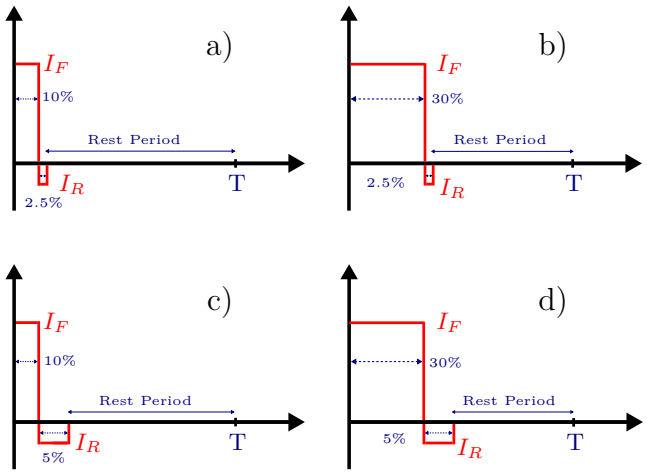

Figure 9. Example of AC waveforms with a reverse period and different duty cycles.

interrupted current signal with 10% duty cycle at 100Hz.

The choice of the current density is particularly critical in the third solution: if it is too high, an insoluble blue oxide will tend to form (see fig.10), while if it is too low it will cause a build up of copper in the bath that will eventually modify its composition. Current interruption, current reversal and ultrasonic agitation are expected to increase the permissible current density range [9]. Without proper agitation, brownish deposit results.

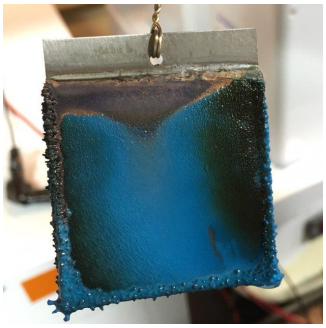

Figure 10. Example of insoluble blue oxide formed in the third step when the current density is too high. In this case j=50mA cm^{-2}.

3.2.2 Charge Density

According to Faraday's law, the amount of electrochemical reaction that occurs at an electrode (the weight of the deposited material w) is proportional to the quantity of electric charge Q passed through the electrochemical cell:

$$w = ZQ = ZIt \tag{6}$$

Z is the so called *electrochemical equivalent* and t is the deposition time. The electrochemical equivalent of a metal is the weight in grams produced/removed by one Coulomb in a redox reaction, and can be calculated

as the ratio of one weight equivalent over the Faraday's constant:

$$Z = \frac{w_{eq}}{F} = \frac{A_{wt}}{zF} = \\ = \frac{g \cdot \mathrm{mol}^{-1}}{\#\text{ of electrons involved} \cdot C \cdot \mathrm{mol}^{-1}} = g \cdot C^{-1} \tag{7}$$

Assuming that deposition occurs just on one face of the sample, the deposit thickness may be evaluated from the volume and the density d of the deposit once the deposition time is known. Being A the plated surface area, the thickness h of the deposit after a time t is given by

$$h = \frac{V}{A} = \frac{w}{dA} = \frac{ZQ}{Ad} = \frac{Z\sigma}{d}, \tag{8}$$

where σ is the total charge density transferred to the sample. Obviously, when considering 3D materials, things get more complicated, but still a relation between the final thickness of the deposit and the total charge density will be conserved. Also, part of the current provided to the cell will be used in side processes (i.e. hydrogen reduction) so that current efficiency is always below 100%, but the evaluation of such effects is beyond the aim of the present project.

However, what we did was not to check the relation $h(\sigma_i)$ for each step $i = 1, 2, 3$. Instead, we fixed the ratios between the charge density in the second step and the ones in the other steps based on the superconducting properties of previous year samples and then looked at the thickness of the superconducting phase formed after the heat treatment as a function of σ_2.

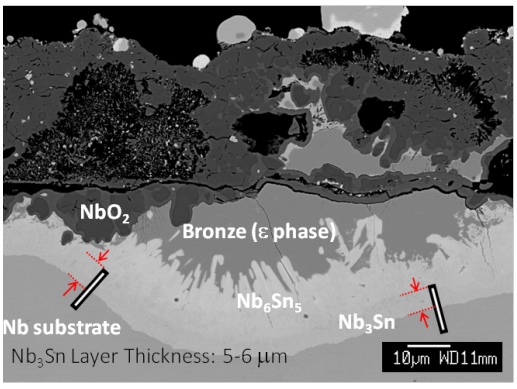

Figure 11. EPMA analysis of sample R10.

As it can be seen from fig.16, sample R10 had the best behaviour in terms of critical temperature. However, measurements of critical field performed at NIMS in Japan showed that samples R22 and R23 had the higher H_{c1}: $500Oe$ and $475Oe$ respectively. Sample R10 only reaches $400Oe$ (see fig.12 and fig.13). Since what really

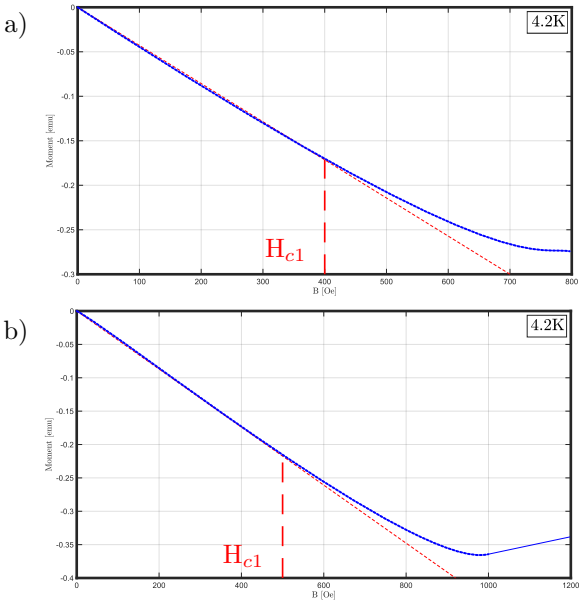

Figure 12. SQUID measurements of critical fields for samples a) R10, H_{c1}=$400Oe$ and b) R22, H_{c1}=$500Oe$. They actually refer to tapes cut out from the bottom of the samples.

matters in SRF applications is the critical magnetic field, that determines the maximum accelerating gradient, we decided to fix $\sigma_2/\sigma_1 \approx 6$ and $\sigma_3/\sigma_2 \approx 2$ according to R22 and R23 recipe in most samples. Also, according to EPMA analysis performed at NIMS, non superconducting phases such as Nb_6Sn_5 were present after the heat treatment on R10 (see fig.11).
At the end of the project we also realized samples according to the recipe of R10 ($\sigma_2/\sigma_1 \approx 8$ and $\sigma_3/\sigma_2 \approx 1.3$), but there was no time to test them.

The first sample that showed superconducting properties was D28. In this case we set $\sigma_2 = 260\mathrm{mC\,cm}^{-2}$ and obtained a Nb_3Sn layer of $h_s = (5.86 \pm 1.55)\mu\mathrm{m}$. The second one, D29, was realized by doubling the charge density in the second step and scaling the other two accordingly. In this case we got $h_s = (11.77 \pm 5.57)\mu\mathrm{m}$, confirming that a linear relation between h_s and σ_2 is a good approximation. SEM/EDS images of the superconducting phase are shown in fig.14 and fig.15 respectively.
Even if the Nb_3Sn layer seems to be quite uniform this is only a small portion of one side of the sample. Indeed, such uniform islands alternate to less defined regions along the samples.

The critical temperatures of D28 and D29 were extremely similar, meaning that T_c is a quite robust property with respect to thickness variations. Also, it was in good agreement with the critical temperatures obtained last year: better than R23, worse than R10 and almost identical to R22 (see fig.16). On the other hand, the curves

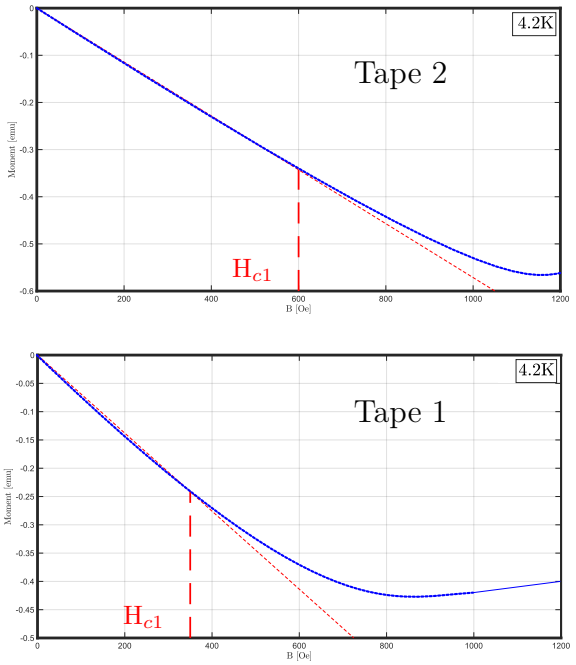

Figure 13. SQUID measurements of critical fields for sample R23. They actually refer to tapes cut out from the bottom of the samples. For sample R23 the values from two tapes have been averaged: the first at the bottom (H_{c1}=350Oe) and the second immediately above (H_{c1}=600Oe).

showing the critical current density J_c *vs* the applied magnetic field B turned out to be significantly different (see fig.17). Even if D28 has a Nb_3Sn layer which is only half of the one of D29, it is able, at 14T, to withstand a current which is almost doubled (this means a factor of 4 in the ratio between the current densities). However, at lower fields, D28 quenches to its normal state showing no transition, confirming the dependence of the instability of Nb_3Sn films on the product $J_c \cdot h$.

3.2.3 Electrodes Position and Geometry

The result of every deposition step also depends on the electrodes shape and reciprocal distance.
If the anode surface is too small compared to the surface to be plated, then, as a consequence of side reactions or impurities in the solution, a layer of oxide will form on its surface preventing further deposition. Oxidation starts in a region corresponding to the shape of the cathode and then extends itself. This is clear from fig.18 where a copper electrode after the first step is shown. As a consequence, it is not recommended to use a large deposition time since the quality of the deposit will decreases the more oxide is formed.
That is why it is highly recommended to use oxygen free anodes having a surface area ratio with respect to the substrate of at least 2:1. At first we tried to use anodes with the same dimensions of the cathode in order to produce current flux lines as homogeneous as possible. Nevertheless, in this way the voltage across the

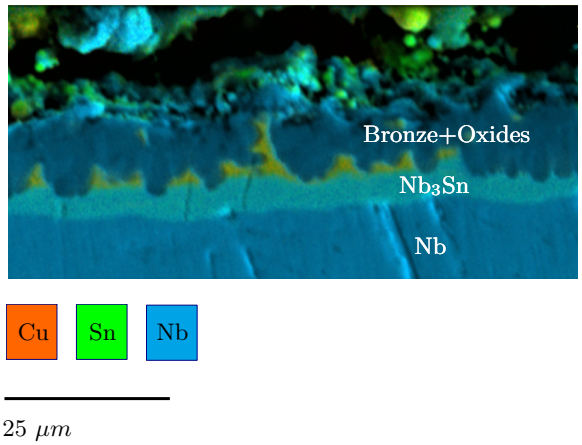

Figure 14. Cross section of sample D28 after the heat treatment. It is possible to see that along with bronze, Nb oxides also form on the outer surface.

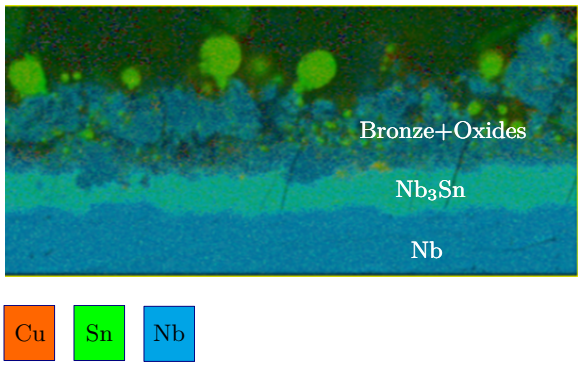

Figure 15. Cross section of sample D29 after the heat treatment. It is possible to see that along with bronze, Nb oxides also form on the outer surface.

electrochemical cell started to increase before deposition was concluded, indicating the presence of the additional impedance in series to the circuit due to the oxide growth.

Moreover, the position of the anodes with respect to the substrate modifies the the diffusion layer and, according to (4), the limiting current density. As a consequence, the same current density will produce a different deposit for different electrodes configurations (i.e. single anode *vs* double anodes). Ideally when two anodes are used, as in the top of fig.4, then deposition should be identical on both faces of the sample. In practice this is never the case because of misalignments and voltage drops across the external interconnections.
A similar effect is produced by the distance between the anodes and the substrate. At smaller distances the deposition rate increases as well as the risk of dentritic deposit since the diffusion layer gets replenished faster. We fixed the current density at a reasonably low value to

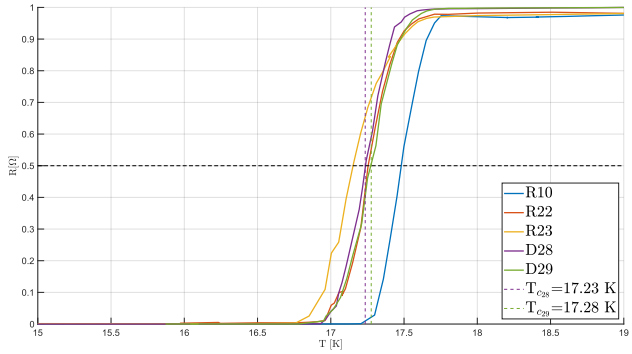

Figure 16. Comparison between resistance *vs* temperature curves of most representative samples. Measuremens have been performed on a 1cm wide tape cut out from the bottom of each sample.

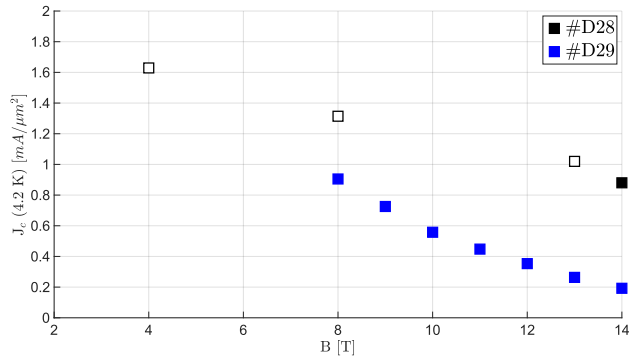

Figure 17. Comparison between critical current curves of samples D28 and D29 at 4.2K. Measurements have been performed on a 1cm wide tape cut out from the bottom of each sample. To estimate the cross section of the superconducting layer the double of the average thickness resulting from SEM observations have been used.

be away from j_L (from dentritic deposit in practice) and then we varied the electrodes distance so as to obtain a good homogeneity.
It turned out that 25mA cm^{-2} applied with a distance of 2cm between the electrodes (top of fig.4 for the set up), produce the best result for both rectangles and disks. The set up used for cylinder was different (see bottom of fig.4) since the idea was to make the cylinder to fit the mold used to take SEM images. This imposed a maximum diameter of 3cm for the cylinder. Since the anodic rods had a diameter of 1cm this produced a distance from the cathode of only 1cm. We tried to find the optimal value for the current density also in this case, but we only had time to set an upper bound of 18.72mA cm^{-2}, which still produced rough deposit.
However, also the opposite could be done, fixing the distance and then varying the current density, but the limits of the current supply should be taken into account in that case. The structure that has been used is shown in fig.19.

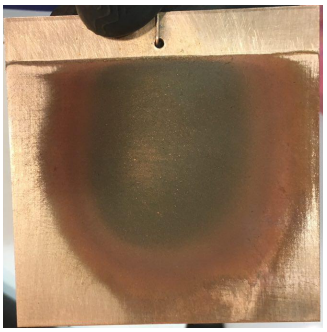

Figure 18. Copper electrode after the first deposition step on a disk sample. Oxidation starts in a region corresponding to the "image" of the substrate and then extends to the surrounfings.

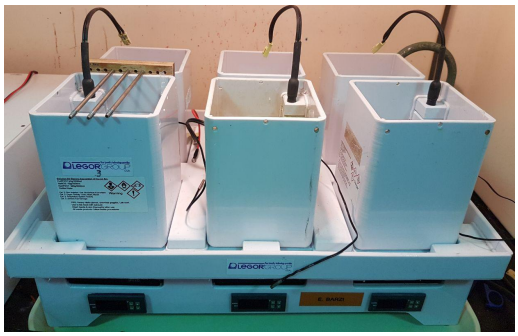

Figure 19. Electrodes configuguration in the last structure that was used (a few were tried before this).

3.2.4 Substrate Surface Roughness

All the above information would still be unknown to us and this paper would not have been written in this way if we had got right the following issue: **substrate roughness**. It causes the crisis at the origin of all our investigations.

The main issue of last year samples was the roughness of the resulting Nb_3Sn layer. Looking at a cross section using SEM (see fig.20), valleys with a depth of the order of 10µm were present. The problem was that when

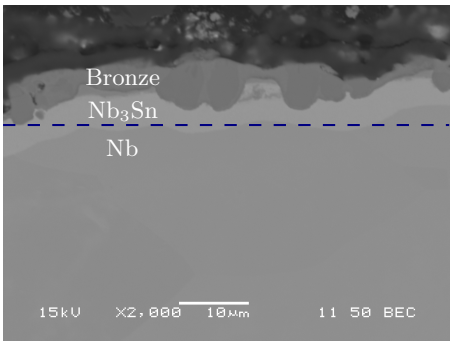

Figure 20. Cross section image of a disk sample at SEM with backscattered electrons. The Nb_3Sn layer is the brightest one, which is to say the heaviest. If one attempted to remove the outer bronze layer (the one just above Nb_3Sn) by polishing up to the dashed line, then most of the superconducting layer would be removed.

trying to remove the outer bronze and level out the surface[8], there was the risk of creating discontinuities in the superconducting layer and to remove almost all of it.
As a consequence, the niobium foils for this year were prepared with the lowest possible roughness. Also, some electropolished samples were ordered from KEK. The corresponding roughness, measured with a laser confocal microscope at 20x magnification, are shown in fig.21. In order to preserve the existing roughness we did not perform any mechanical grinding on the substrates and oxides removal was entrusted only to the HF rinsing: this was deleterious. All samples we prepared turned out to be non superconductive. We tried different solutions and discovered a number of process parameters and characteristics (the one listed above) that were neglected in last year analysis.

Still, we did not get any result until we performed deposition on KEK samples, that were the most promising one. Soon after the end of the third step we observed a total delamination of the deposit: the first copper layer did not adhere at all (see fig.22).

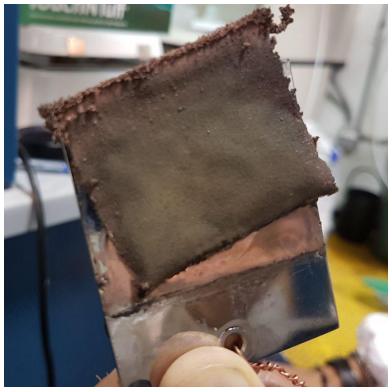

Figure 22. Delamination of the deposit from the KEK's electropolished sample.

What was missing in our analysis was a physical explanation of the growth mechanism behind electrodeposition. Indeed the absorption of ions and the layer growth start in correspondence of surface defects such as vacancies, kink sites or grain boundaries, and the more the surface is smooth the less the deposit will adhere.
Probably, what happened in the first samples is that, during the heat treatment, most of the deposit did not react with the niobium substrate but felt off because of the poor adhesion.

After that, we started grinding all niobium substrates with Scotch-Brite 7447 before rinsing them in HF, so as to provide more nucleation points. The first we reacted, D28, was superconductive.
The problem related to the removal of the bronze layer can be solved by increasing the thickness of the Nb_3Sn layer (that is directly proportional to the charge density transferred to the substrate during the second deposition step), so as to leave margin for future ad-hoc etching/polishing techniques.

In Table 2 it is shown the history of the project along with the process parameters of each sample. It is possible to notice how we evolved from a repetition of the last year work to a much more standardized technique.

4 FUTURE RESEARCH

The next steps of the present work are basically two:

- Find a recipe which is able to optimize the superconducting properties of the Nb_3Sn layer. This basically implies to tune the ratios between the charge densities σ_2/σ_1 and σ_3/σ_2. Moreover, adjustment to the set-up maybe done. New electrodes (oxides free) and enhanced electrolytic solutions may be used to reduce oxides formation. Also the time required for the deposition may be reduced with a configuration using larger (or more) electrodes and many substrates connected in series;

- Transfer the technique from flat to curved surfaces and ultimately to cavities. Curved surfaces might be a critical issue since additional stresses develops in the layer that could destroy the superconducting properties. We tried deposition on cylinders and the results were quite promising (see fig.23), but we did not have time to react and test them.
Concerning deposition on real cavities it could be possible, by controlling the shape of the electrode and the flow of the electrolyte, to ensure a quite uniform deposit on the inner surface. A possible idea to do this is shown in fig.24.

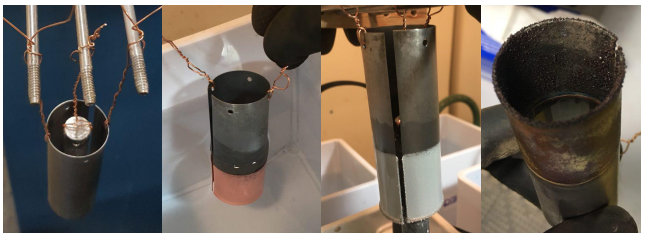

Figure 23. The set-up of the electrochemical cell and the deposition steps on a cylindrical sample. Brownish deposit appear as a consequence of poor agitation.

[8] A certain limit to the surface roughness is imposed in SRF cavity applications, even if just a 2 µm thick layer is required.

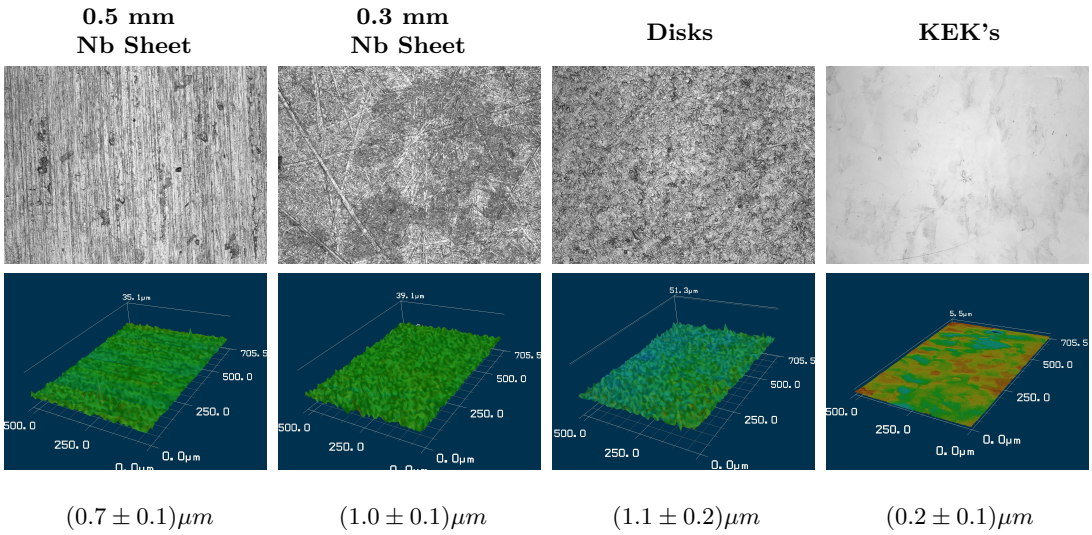

Figure 21. The average roughness of each Nb foil is shown. The samples from KEK have the lowest value, as it can be also seen from the laser images on the top.

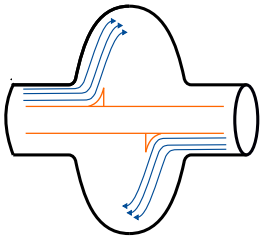

Figure 24. In order to perform uniform deposition on the inner surface of a cavity, a cylindrical anodes with two steps on top of it might be used. By tuning the shape of such steps and the flux velocity the desired coating might be obtained.

Table 1 Charge density parameters of most relevant last year samples. S_a and S_c are the surface of the anode and the cathode respectively. In that case the electrodes had three different shapes, and that is the reason why three different ratios S_a/S_c are reported.

2017 SAMPLES	R10	R22	R23
σ_1 [mC/cm^2]	35.00	42.00	40.00
σ_2 [mC/cm^2]	290.00	260.00	240.00
σ_3 [mC/cm^2]	380.00	454.00	455.00
σ_2/σ_1	8.29	6.19	6.00
σ_3/σ_2	1.31	1.75	1.90
$(S_a/S_c)_1$	0.35	1.05	1.31
$(S_a/S_c)_2$	1.21	3.70	4.60
$(S_a/S_c)_3$	0.35	1.05	1.31

REFERENCES

[1] S Posen and D L Hall. Nb_3sn superconducting radiofrequency cavities: fabrication, results, properties, and prospects. *Superconductor Science and Technology*, 30(3):033004, 2017.

[2] E Barzi, M Bestetti, F Reginato, D Turrioni, and S Franz. Synthesis of superconducting Nb_3Sn coatings on Nb substrates. *Superconductor Science and Technology*, 29(1):015009, 2016.

[3] Stefano Falletta. Optimization of Superconducting Nb_3Sn Electrochemical Film Technologies. 2017.

[4] Reginato F. Electrochemical synthesis of nb–sn coatings for high field accelerator magnets. *Laurea Thesis, Politecninco di Milano*, 2014.

[5] Paunovic M. Schlesinger, M. Modern electroplating. *Handbook of Deposition Technologies for Films and Coatings—Science, Technology and Applications*, page 729, 2010.

[6] Morton Schwartz. Deposition from aqueous solutions: an overview. *Handbook of Deposition Technologies for Films and Coatings—Science, Technology and Applications*, page 506, 1994.

[7] James T. Hinatsu and Frank R. Foulkes. Diffusion coefficients for copper (ii) in aqueous cupric sulfate-sulfuric acid solutions. 136(1):125–132, 1989.

[8] Robert Walker and Nicholas S. Holt. Determination of the nernst diffusion layer thickness in the hydroson agitation tank. *Surface Technology*, 22(2):165 – 174, 1984.

[9] Dr. Donald Snyder. Choosing and troubleshooting copper electroplating processes. 2017.

Table 2 Here is the list of all samples that were realized during the project along with the corresponding process parameters. Samples that were not grinded before deposition were not superconductive. Unfortunately there was time to test only samples D28 and D29 before the end of the internship. A summary of the parameters related to the charge density in past samples is provided in Table 1.
Length and width measurements are affected by an uncertainty of approximately 0.2cm since the surface that was actually in the solution was not so easy to be controlled with the actual set-up (this is why the heights are quite different from each other). Thickness measurements were instead performed with an micrometer and therefore their uncertainty can be taken to be 1µm. $\delta_{time} \approx 0.1s$ and $\delta_T \approx 3°C$.
The parameter h for Disks represent the height of the circular segment that is not immersed in the solution. S_a and S_c are the surface of the anode and the cathode respectively. d is the distance between anode/s and cathode.
The cathode current density J was provided by a DPR20-15-30XR Dynatronix pulse powers supply.

RECTANGLES	Nb SAMPLE				Cu, Sn ELECTRODES					ELECTRODEPOSITION PARAMETERS														
#	l [cm]	w [cm]	t [cm]	S_c[cm^2]	l [cm]	w [cm]	t [cm]	S_a[cm^2]	Geometry	$S_{a,tot}/S_c$	d [cm]	Grind Sample	Step	J [mA/cm^2]	time [min]	σ [mC/cm^2]	σ_2/σ_1	σ_3/σ_2	I_{av} [A]	I_F [A]	T [ms]	DC_F [%]	T [°C]	$time_{HF}$ [min]
													1	21.00	2.00	42.00			1.274				40	
R24	10.000	3.000	0.03	60.69	13.000	2.500	0.10	67.85	| | |	2.24	5.50	No	2	37.00	15.00	555.00	13.21	0.86	2.246	13.42 F. -2,68 R	10.00	10% F, 2.5% R	50	5.00
													3	16.00	30.00	480.00			0.971				50	
													1	21.00	2.00	42.00			0.893				40	
R25	7.000	3.000	0,03	42,51	13,000	2,500	0,10	67,85	| | |	3,19	5,50	No	2	37,00	15,00	555,00	13,21	0,86	1,573	3,03 F, -0,61 R	10,00	30% F, 2.5% R	50	5,00
													3	16.00	30.00	480.00			0.680				50	
													1	21.00	2.00	42.00			0.893				40	
R26	7.000	3.000	0.03	42.51	13.000	2.500	0.10	67.85	| | |	3.19	5.50	No	2	37.00	15.00	555.00	13.21	0.86	1.573	9.92 F, -1.98 R	10.00	10% F, 5% R	50	5.00
													3	16.00	30.00	480.00			0.680				50	
													1	21.00	4.00	84.00			1.187				40	
R27	7.000	4.000	0.03	56.54	13.000	2.500	0.10	67.85	| | |	2.40	5.50	No	2	37.00	15.00	555.00	6.61	0.86	2.092	4.09 F, -0.82 R	10.00	30% F, 5% R	50	5.00
													3	16.00	30.00	480.00			0.905				50	
													1	21.00	4.00	84.00			0.900				40	
R28	7.000	3.000	0.05	42.85	13.000	2.500	0.10	67.85	| | |	3.17	5.50	No	2	37.00	15.00	555.00	6.61	1.73	1.585	3.05 F, -0.61 R	10.00	30% F, 2.5% R	50	5.00
													3	16.00	60.00	960.00			0.686				50	
													1	40.00	4.00	160.00			1.626	16.26	10.00	10	40	
R29	4.000	5.000	0.05	40.65	4.000	5.000	0.10	41.30	| | |	2.03	5.50	No	2	60.00	15.00	900.00	5.63	1.00	2.439	24.39	10.00	10	50	5.00
													3	30.00	30.00	900.00			1.220	12.20	10.00	10	50	
													1	20.00	8.00	160.00			0.813	8.13	10.00	10	40	
R30	4.000	5.000	0.05	40.65	4.000	5.000	0.10	41.30	| | |	2.03	5.50	No	2	30.00	30.00	900.00	5.63	0.25	1.220	12.20	10.00	10	50	5.00
													3	15.00	15.00	225.00			0.610	6.10	10.00	10	50	
													1	60.00	1.40	84.00			1.449	14.49	10.00	10	40	
R31	4.000	2.950	0.050	24.148	6.500	8.000	0.15	107.15	| | |	8.87	2.00	Yes	2	50.00	10.40	520.00	6.19	3.46	1.207	12.07	10.00	10	50	5.00
													3	60.00	30.00	1800.00			1.449	14.49	10.00	10	50	
													1	60.00	1.40	84.00			1.449	14.49	10.00	10	40	
R32	4.000	2.950	0.050	24.148	6.500	8.000	0.15	107.15	| | |	8.87	2.00	Yes	2	50.00	10.40	520.00	6.19	5.19	1.207	12.07	10.00	10	50	5.00
													3	60.00	45.00	2700.00			1.449	14.49	10.00	10	50	
													1	60.00	2.80	168.00			1.956	19.56	10.00	10	40	
R33	4.000	4.000	0.050	32.600	6.500	8.000	0.15	107.15	| | |	6.57	2.00	Yes	2	50.00	20.80	1040.00	6.19	1.74	1.630	16.30	10.00	10	50	0.00
													3	50.00	36.27	1813.50			1.630	16.30	10.00	10	50	
													1	32.57	4.20	136.79			1.141	11.41	10.00	10	40	
R34	4.300	4.000	0.050	35.030	6.500	8.000	0.15	107.15	| | |	6.12	2.00	Yes	2	32.57	26.00	846.82	6.19	1.74	1.141	11.41	10.00	10	50	0.00
													3	32.57	45.33	1476.40			1.141	11.41	10.00	10	50	
													1	32.96	4.20	138.43			1.141	11.41	10.00	10	40	
R35	4.250	4.000	0.050	34.625	6.500	8.000	0.15	107.15	| | |	6.19	2.00	Yes	2	32.96	26.00	856.96	6.19	1.74	1.141	11.41	10.00	10	50	0.00
													3	32.96	45.33	1494.08			1.141	11.41	10.00	10	50	
													1	33.75	3.14	105.98			1.141	11.41	10.00	10	40	
R36	4.150	4.000	0.050	33.815	6.500	8.000	0.15	107.15	| | |	6.34	2.00	Yes	2	33.75	26.00	877.50	8.28	1.31	1.141	11.41	10.00	10	50	5.00
													3	33.75	34.00	1147.50			1.141	11.41	10.00	10	50	
													1	26.97	3.66	98.71			0.978	9.78	10.00	10	40	
R37	4.450	4.000	0.050	36.245	6.500	8.000	0.15	107.15	| | |	5.91	2.00	Yes	2	26.97	30.33	818.00	8.29	1.31	0.978	9.78	10.00	10	50	5.00
													3	26.97	39.66	1069.63			0.978	9.78	10.00	10	50	
													1	24.10	4.40	106.04			0.815	8.15	10.00	10	40	
R38	4.150	4.000	0.050	33.815	6.500	8.000	0.15	107.15	| | |	6.34	2.00	Yes	2	24.10	36.40	877.24	8.27	1.31	0.815	8.15	10.00	10	50	5.00
													3	24.10	47.60	1147.16			0.815	8.15	10.00	10	50	
DISKS	**Nb SAMPLE**				**Cu, Sn ELECTRODES**					**ELECTRODEPOSITION PARAMETERS**														
#	r [cm]	h [cm]	t [cm]	S_c[cm^2]	l [cm]	w [cm]	t [cm]	S_a[cm^2]	Geometry	$S_{a,tot}/S_c$	d [cm]	Grind Sample	Step	J [mA/cm^2]	time [min]	σ [mC/cm^2]	σ_2/σ_1	σ_3/σ_2	I_{av} [A]	I_F [A]	T [ms]	DC_F [%]	T [°C]	$time_{HF}$ [min]
													1	20.00	2.00	40.00			0.791	7.91	10.00	10	40	
D20	2.475	0.500	0.250	39.543	2.475	0.500	0.250	39.543	| | |	2.00	5.50	No	2	35.00	7.00	245.00	6.13	1.84	1.384	13.84	10.00	10	50	5.00
													3	15.00	30.00	450.00			0.593	5.93	10.00	10	50	
													1	20.00	4.00	80.00			0.791	7.91	10.00	10	40	
D21	2.475	0.500	0.250	39.543	2.475	0.500	0.250	39.543	| | |	2.00	5.50	No	2	35.00	14.00	490.00	6.13	0.92	1.384	13.84	10.00	10	50	5.00
													3	15.00	30.00	450.00			0.593	5.93	10.00	10	50	
													1	40.00	4.00	160.00			1.582	15.82	10.00	10	40	
D23	2.475	0.500	0.250	39.543	6.500	8.000	0.15	107.15	| |	2.71	5.50	No	2	70.00	14.00	980.00	6.13	0.92	2.768	27.68	10.00	10	50	5.00
													3	30.00	30.00	900.00			1.186	11.86	10.00	10	50	
													1	53.33	4.00	213.32			2.109	21.09	10.00	10	40	
D25	2.475	0.500	0.250	39.543	6.500	8.000	0.15	107.15	| |	2.71	5.50	No	2	64.81	14.00	907.34	4.25	1.00	2.563	25.63	10.00	10	50	5.00
													3	30.35	30.00	910.50			1.200	12.00	10.00	10	50	
													1	63.21	2.00	126.42			2.500	25.00	10.00	10	40	
D26	2.475	0.500	0.250	39.543	6.500	8.000	0.15	107.15	| |	2.71	5.50	No	2	75.87	10.00	758.70	6.00	1.33	3.000	30.00	10.00	10	50	5.00
													3	50.57	20.00	1011.40			2.000	20.00	10.00	10	50	
													1	50.00	4.00	200.00			1.841	18.41	10.00	10	40	
D27	2.475	0.500	0.030	36.826	6.500	8.000	0.15	107.15	| | |	5.82	2.00	Yes	2	60.00	10.00	600.00	3.00	_	2.210	22.10	10.00	10	50	5.00
													3	-	-	-			-	-	10.00	10	50	
													1	60.00	0.70	42.00			2.210	22.10	10.00	10	40	
D28	2.475	0.500	0.030	36.826	6.500	8.000	0.15	107.15	| | |	5.82	2.00	Yes	2	50.00	5.20	260.00	6.19	1.74	1.841	18.41	10.00	10	50	5.00
													3	60.00	7.56	453.60			2.210	22.10	10.00	10	50	
													1	60.00	1.40	84.00			2.210	22.10	10.00	10	40	
D29	2.475	0.500	0.030	36.826	6.500	8.000	0.15	107.15	| | |	5.82	2.00	Yes	2	50.00	10.40	520.00	6.19	1.74	1.841	18.41	10.00	10	50	5.00
													3	60.00	15.12	907.20			2.210	22.10	10.00	10	50	
													1	34.99	2.80	97.97			1.186	11.86	10.00	10	40	
D30	2.475	1.200	0.250	33.897	6.500	8.000	0.15	107.15	| | |	6.32	2.00	Yes	2	34.89	17.33	604.64	6.17	1.74	1.183	11.83	10.00	10	50	5.00
													3	34.89	30.24	1055.07			1.183	11.83	10.00	10	50	
													1	31.12	2.80	87.14			1.186	11.86	10.00	10	40	
D31	2.475	0.700	0.250	38.099	6.500	8.000	0.15	107.15	| | |	5.62	2.00	Yes	2	31.12	17.33	539.31	6.19	1.74	1.186	11.86	10.00	10	50	5.00
													3	31.12	30.24	941.07			1.186	11.86	10.00	10	50	
													1	33.25	2.80	93.10			1.186	11.86	10.00	10	40	
D32	2.475	1.000	0.250	35.663	6.500	8.000	0.15	107.15	| | |	6.01	2.00	Yes	2	33.25	17.33	576.22	6.19	1.74	1.186	11.86	10.00	10	50	5.00
													3	33.25	30.24	1005.48			1.186	11.86	10.00	10	50	
													1	30.82	2.80	86.30			1.186	11.86	10.00	10	40	
D33	2.475	0.650	0.250	38.475	6.500	8.000	0.15	107.15	| | |	5.57	2.00	Yes	2	30.82	17.33	534.11	6.19	1.74	1.186	11.86	10.00	10	50	5.00
													3	30.82	30.24	932.00			1.186	11.86	10.00	10	50	
													1	31.60	2.80	88.48			1.186	11.86	10.00	10	40	
D34	2.475	0.650	0.170	37.524	6.500	8.000	0.15	107.15	| | |	5.71	2.00	Yes	2	31.60	17.33	547.63	6.19	1.74	1.186	11.86	10.00	10	50	
													3	31.60	30.24	955.58			1.186	11.86	10.00	10	50	
													1	28.00	3.00	84.00			1.067	10.67	10.00	10	40	5.00
D35	2.475	0.700	0.250	38.099	6.500	8.000	0.15	107.15	| | |	5.62	2.00	Yes	2	28.00	18.57	519.96	6.19	1.74	1.067	10.67	10.00	10	50	
													3	28.00	32.40	907.20			1.067	10.67	10.00	10	50	
													1	24.51	3.36	82.35			0.952	9.52	10.00	10	40	5.00
D36	2.475	0.600	0.250	38.841	6.500	8.000	0.15	107.15	| | |	5.52	2.00	Yes	2	24.51	20.80	509.81	6.19	1.74	0.952	9.52	10.00	10	50	
													3	24.51	36.28	889.22			0.952	9.52	10.00	10	50	
													1	24.51	3.36	82.35			0.952	9.52	10.00	10	40	5.00
D37	2.475	0.600	0.250	38.841	6.500	8.000	0.15	107.15	| | |	5.52	2.00	Yes	2	24.51	20.80	509.81	6.19	1.74	0.952	9.52	10.00	10	50	
													3	24.51	36.28	889.22			0.952	9.52	10.00	10	50	
													1	26.08	3.36	87.63			0.952	9.52	10.00	10	40	5.00
D38	2.475	0.900	0.250	36.506	6.500	8.000	0.15	107.15	| | |	5.87	2.00	Yes	2	26.08	20.80	542.46	6.19	1.74	0.952	9.52	10.00	10	50	
													3	26.08	36.28	946.18			0.952	9.52	10.00	10	50	
													1	24.08	3.36	80.91			0.952	9.52	10.00	10	40	5.00
D39	2.475	0.500	0.250	39.543	6.500	8.000	0.15	107.15	| | |	5.42	2.00	Yes	2	24.08	20.80	500.86			0.952	9.52	10.00	10	50	
													3	24.08	36.28	873.62			0.952	9.52	10.00	10	50	
CYLINDERS	**Nb SAMPLE**				**Cu, Sn ELECTRODES**					**ELECTRODEPOSITION PARAMETERS**														
#	r_{in} [cm]	h [cm]	t [cm]	S_c[cm^2]	l [cm]	w [cm]	t [cm]	S_a[cm^2]	Geometry	$S_{a,tot}/S_c$	d [cm]	Grind Sample	Step	J [mA/cm^2]	time [min]	σ [mC/cm^2]	σ_2/σ_1	σ_3/σ_2	I_{av} [A]	I_F [A]	T [ms]	DC_F [%]	T [°C]	$time_{HF}$ [min]
													1	45.00	2.00	90.00			2.583	25.83	10.00	10	40	
C1	1.500	3.000	0.030	57.400	0.750	6.660	_	33.152	Concentric	0.58	0.75	Yes	2	45.00	12.00	540.00	6.00	3.33	2.583	25.83	10.00	10	50	5.00
													3	45.00	40.00	1800.00			2.583	25.83	10.00	10	50	
													1	24.19	3.36	84.00			1.435	14.35	10.00	10	40	
C2	1.500	3.100	0.030	57.400	0.750	6.660	_	33.152	Concentric	0.58	0.75	Yes	2	24.19	20.80	520.00	6.19	1.74	1.435	14.35	10.00	10	50	5.00
													3	24.19	36.28	907.00			1.435	14.35	10.00	10	50	
													1	21.42	4.20	84.00			1.148	11.48	10.00	10	40	
C3	1.500	2.800	0.030	57.400	0.750	6.660	_	33.152	Concentric	0.58	0.75	Yes	2	21.42	26.00	520.00	6.19	1.74	1.148	11.48	10.00	10	50	5.00
													3	21.42	45.35	907.00			1.148	11.48	10.00	10	50	
													1	18.72	5.60	84.00			1.148	11.48	10.00	10	40	
C4	1.500	2.400	0.030	57.400	0.750	6.660	_	33.152	Concentric	0.58	0.75	Yes	2	18.72	34.66	520.00	6.19	1.74	1.148	11.48	10.00	10	50	5.00
													3	18.72	60.67	907.00			1.148	11.48	10.00	10	50	